Eike Schling, Zongshuai Wan, Hui Wang, Pierluigi D'Acunto

Asymptotic Geodesic Hybrid Timber Gridshell

Abstract: This paper presents a strategy to design and build strained timber gridshells from exclusively straight timber planks, which are interwoven and elastically deployed into a doubly curved web. For this purpose, we combine asymptotic (A) and geodesic (G) curves into hybrid AAG-webs on curved surfaces. We present a digital method to design and geometrically optimize the timber AAG-webs to include equal intersection angles and geodesic boundaries. This new construction system benefits from the targeted use of the two differing bending axes of timber planks for flexibility and rigidity. The flat geodesic planks are interlaced at the midpoint of the asymptotic beams to create a tri-hex pattern, which lowers the buckling length and decisively increases the overall stiffness. As a proof of concept, a large-scale timber gridshell covering an area of 60 m^2 was designed and built. We document the construction process of manufacturing, prefabrication, elastic deformation, on-site assembly, and installation of the polycarbonate cover to verify constructive tolerances and feasibility. The structure is tested and simulated to validate our computational results.

Keywords: asymptotic curves, geodesic curves, timber gridshells, elastic bending and torsion, curvature analysis, timber AAG-webs, resistance through form, cradle-to-cradle

1 Introduction

The construction industry is one of the biggest contributors to environmental degradation and CO_2 emissions. Construction waste can be avoided by using standardized elements that can be disassembled and reused in the future. This cradle-to-cradle approach seems to be incompatible with the idea of freeform design, which usually demands highly bespoke elements and complex fabrication. Our research is looking to resolve this contradiction, by exploring the design and fabrication of doubly curved gridshells from exclusively flat and straight, off-the-shelf timber planks with repetitive joints. This offers substantial material savings compared to CNC-milled lattice gridshells. The flat packed planks can be transported easily, which in turn reduces CO_2 emissions, and assembled utilizing the kinetic behaviour of lamella grids.

1.1 Geometrical background

Architectural Geometry has introduced methods to control and optimize doubly curved surfaces (Pottmann et al. 2007). The curvature $\kappa = |c''(s)|$ of a curve $c(s)$ (with arc length parameter s) on a surface S is decomposed into two parts i. e. normal curvature κ_n and geodesic curvature κ_g, which are the two projections of the curvature vector

https://doi.org/10.1515/9783111162683-008

c'' onto the surface normal and tangent plane at a surface point (Fig. 1a). These three curvature elements have the relation $\kappa^2 = \kappa_n^2 + \kappa_g^2$. Let α be the angle between c'' and the surface normal, then $\kappa_n = \kappa\cos(\alpha)$, $\kappa_g = \kappa\sin(\alpha)$. The value of constant α throughout the curve has two special cases ($\pi/2$ and 0), making two special kinds of curves on the surface. When $\alpha = \pi/2$ along the curve, it characterizes an *asymptotic curve* with $\kappa_n = 0$, and the curvature vectors lie on the tangent planes. If $\alpha = 0$, then it is a *geodesic curve* with $\kappa_g = 0$, and the curvature vectors are in the planes spanned by the tangents and surface normals. By constraining either κ_n or κ_g to zero, we can design gridshells that can be built from *straight asymptotic* or geodesic planks (Fig. 1b,c).

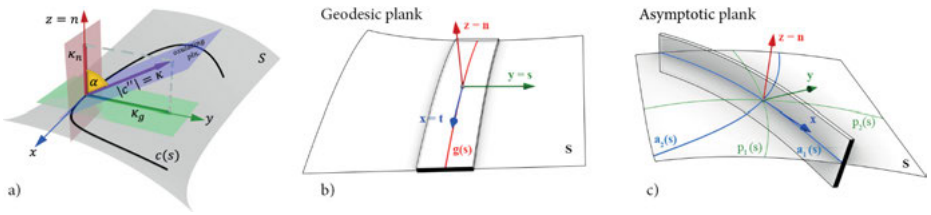

Fig. 1: Curvature of curves and planks: a) Relationship of κ, κ_n and κ_g of a curve $c(s)$ on a surface S. b) Plank along geodesic curve $g(s)$ on a surface S. c) Plank along asymptotic curve $a_1(s)$ on a surface S. Asymptotic curves $a_1(s)$ and $a_2(s)$ are symmetric with respect to the principal curvature lines $p_1(s)$ and $p_2(s)$.

1.2 Geodesic and asymptotic structures

Geodesic and asymptotic planks have, until now, been used independently for the design of gridshells. *Geodesic structures* have been studied (among others) for their construction simplicity and structural performance (Weinand and Pirazzi 2006). Julian Natterer developed Timber gridshells from flat geodesic planks (Natterer et al. 2000), using a technique of layering to create bespoke ribbed shells. Research in Architectural Geometry has investigated versatile geodesic patterns (Pottmann et al. 2010), their self-forming behavior from flat to curved grid (Soriano 2017) as well as their potential to reuse recycled, off-the shelf material (Haskell et al. 2021).

Asymptotic structures have been described through mathematical theory as early as (Finsterwalder 1897). Recently, a higher attention has been paid to asymptotic networks, their developable properties (Tang et al. 2016), and their discrete optimization as quad meshes (Jiang et al. 2020). The first asymptotic gridshell, the INSIDE/OUT pavilion was constructed in stainless steel including diagonal steel (Schling et al. 2018). Asymptotic grids can be assembled on flat ground and deformed into the global design shape without need for formwork, as their movement is restricted by the scissor joints, and the directional bending of planks. This kinetic mechanism has been investigated in depth by (Schikore et al. 2020) and used to design transformable structures, such as the

Kinetic Umbrella. Because the asymptotic curves are locally symmetric to the principal curvature directions, an isothermal asymptotic network can be covered with planar quad panels or developable strips in the diagonal direction (Schling and Wan 2022). The panel strips, however, are curved, i. e., do not naturally follow a geodesic path and can thus not easily be built from straight, off-the-shelf panels.

Structural behavior. For both geodesic and asymptotic structures, the slender planks have an effect on global and local stiffness (Schikore 2023). In geodesic gridshells, the weak axis of a plank lies tangential to the design shape, which significantly lowers its global stiffness and results in buckling out-of-plane of the gridshell. Usually, this is overcome by adding additional layers of planks. Asymptotic gridshell are globally stiffer, as their planks stand upright and can carry loads through their strong axis. However, the slender planks may buckle locally in case of high internal compression or bending (lateral-torsional buckling) (Wan and Schling 2022).

1.3 Contributions and Overview

We implement the design and construction of a triangulated timber gridshell by combining asymptotic (A) and geodesic (G) curves into *hybrid AAG webs* (Schling et al. 2022). The geodesic elements triangulate the grid, halve the buckling length, and offer simple façade solutions with standardized aluminum mullions and developable panels. The structure is assembled from only straight off-the shelf planks, without offcuts, or bespoke boundary elements, with the goal to design for disassembly and reuse. In relation to previous work, this paper presents the following contributions:

- an architectural design workflow to create a variety of initialization meshes
- a custom energy term in the optimization problem to fit specific design constraints
- constructive solutions, realized in a case study, the 60 m^2 Timber Vault

The remainder of this paper is structured as follows. In Sec. 2, we present the computational workflow to design and optimize AAG webs. We start with a negatively curved rotational surface to initialize the design routine. The complex AAG web is then generated through discrete optimization using planar constraints of vertex stars. Additional optimization goals, such as equiangular joints, planar and geodesic boundaries are added to simplify fabrication. In Sec. 3, we present the construction development of the AAG Timber Vault. We describe the curvature analysis and material choice, prefabrication, and assembly, including the installation of a semi-discrete façade from bent polycarbonate panels. In Sec. 4, we highlight the design impact on structural performance. We present a digital simulation and validate it through physical load tests. Finally, in Sec. 5, we reflect on the challenges and potentials of this technology and highlight ongoing research in this field.

2 Computational Design and Optimization

Finding a good starting mesh to optimize an AAG-web is not a trivial problem. It highly depends on the mesh parametrization. We adopt rotational surfaces, in which the principal curvature lines are the parallel circles and meridian curves, and the meridian curves are naturally geodesic. We extract mesh patches from negatively curved rotational surfaces and use them as initial meshes for our optimization approach. This enables quick testing of alternative shapes consisting of one or more rotational surfaces that are cropped, intersected, copied, or flipped to create meaningful shell designs (Fig. 2). These models function as preliminary design options to develop construction strategies, details, and material investigations to a high level (Fig. 3), without relying on the final refined mesh geometry.

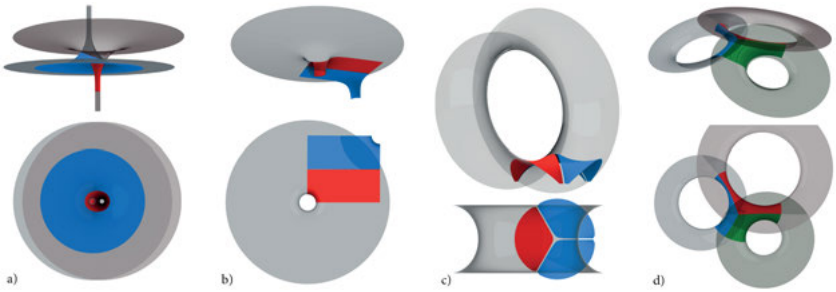

Fig. 2: Designing architectural alternatives with rotational surface (colors differentiate subsequent steps in creation, red, blue and green). a) Flipped rotational surface creating column and roof. b) Cropped rotational surface creating half of the symmetric roof. c) Cropped surface is rotated to create a triple-arched gridshell. d) Three individual rotational surfaces are intersected and cropped to create a vault with three entryways.

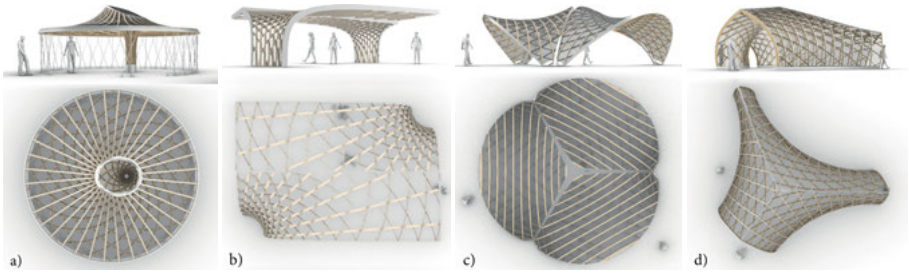

Fig. 3: AAG designs, that are based purely on rotational surfaces. In these cases, joints are not equiangular, and not all boundaries are geodesic. These designs are used to develop architectural ideas quickly without the need for optimization.

2.1 Discrete Nets and Webs

Discrete asymptotic nets (A-nets). The curvature vectors of asymptotic curves lie on the tangent plane of the surface. In a discrete network, three consecutive vertices of an asymptotic polyline define a discrete osculating plane. The mesh is optimized by enforcing that two osculating planes agree at each vertex star (Fig. 4 left). Therefore, a discrete A-net is defined by a quad mesh with planar vertex stars, in which five vertices v_i, $v_{ij}(j = 1, \ldots, 4)$ are coplanar (Sauer 1937, 1970).

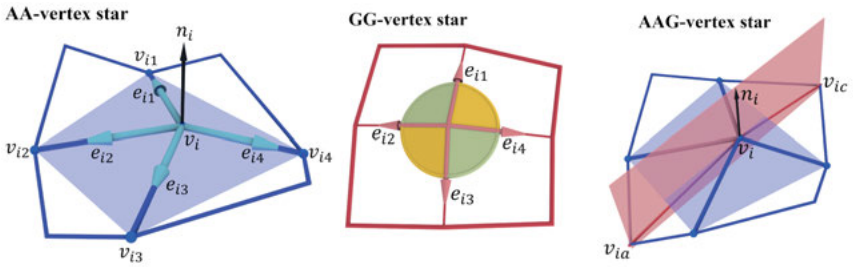

Fig. 4: Left: Planar vertex star of A-net. Middle: Vertex star of a conventional G-net, where two opposite angles are equal. Right: Vertex star of AAG-web, combining a planar vertex-star (AA) with a diagonal plane through the surface normal (G).

Discrete geodesic nets (G-nets) were first introduced by (Wunderlich 1951). A discrete G-net is defined as a quad mesh where two pairs of opposite angles at each vertex star are equal (Fig. 4 middle). However, this angle condition cannot help to get meshes with only one family of geodesic curves.

Discrete asymptotic geodesic nets (AAG-nets). We utilize the geometry property that the discrete osculating plane passes through the surface normals to get the discretization of diagonal geodesics in AAG-webs. The numerical model is achieved by optimization of A-nets with one family of diagonal polylines being geodesic. Depending on the design surface, this logic can be rotated to enforce the asymptotic vertices to be diagonal (see Fig. 4 right).

2.2 AAG optimization

The geometric properties of AAG-webs enable the use of planar rectangular timber strips, which are bent orthogonally on the surface along asymptotic curves and tangentially on the surface along geodesic curves. Numerical optimization is used to simplify the fabrication of the gridshells. To this end, we optimize for constant net angles between asymptotic curves to create repetitive joints. For our timber gridshell design (Fig. 5, 6), we also constrain the bottom boundary curve to be planar and geodesic to simplify the

fabrication of supports. We optimize a symmetric mesh, which is then rotated to form a triple symmetric vault. Below, we list all the constraints as optimization energies we used for our designed shell. Notations refer to Fig. 4. The optimization problem is solved by regularized Gauss-Newton algorithm, where all the geometric conditions are represented by constraints with no more than quadratic equations (Tang et al. 2016).

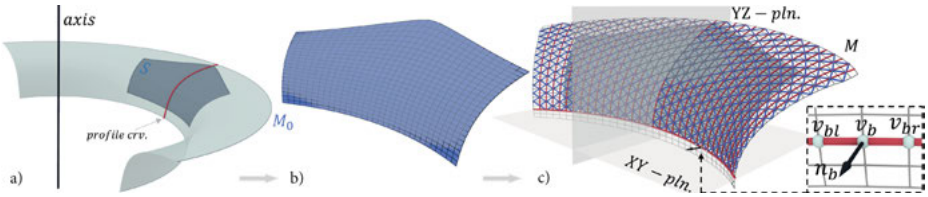

Fig. 5: a) A patch surface S is created from a rotational surface. b) A quad mesh M_0 is rebuilt from S and is used as the initial mesh for optimization. c) An AAG-web MM is achieved by solving the optimization problem with the target function Eq. (7), where one family of mesh polylines are geodesic curves (red), and two diagonal polylines (blue) are asymptotic.

A-net energy. The energy term of A-net is expressed with unit vertex normal n_i of the discrete surface as auxiliary variables. $|V|$ is the number of regular vertex stars, where vertices i are connected by 4 neighboring vertices ij:

$$E_{\text{Anet}} = \sum_{i=1}^{|V|} \sum_{j=1}^{4} \left(n_i \cdot (v_{ij} - v_i)\right)^2 + \sum_{i=1}^{|V|} (n_i \cdot n_i - 1)^2 \tag{1}$$

Geodesic energy. To express the geodesic condition in one of the diagonal directions, we ask for three coplanar vectors $v_{ia} - v_i$, $v_{ic} - v_i$, n_i,

$$E_{\text{geo}} = \sum_{i=1}^{|V|} (n_i \cdot [(v_{ia} - v_i) \times (v_{ic} - v_i)])^2 \tag{2}$$

Angle energy. Given constant angle θ_0 between asymptotic curves, the isogonal condition at each vertex star can be expressed with the help of the unit tangent vectors $t_{i1} = \frac{e_{i1} - e_{i3}}{|e_{i1} - e_{i3}|}$, $t_{i2} = \frac{e_{i2} - e_{i4}}{|e_{i2} - e_{i4}|}$ by $t_{i1} \cdot t_{i2} = \cos\theta_0$, where $e_{ij} = \frac{v_{ij} - v_i}{|v_{ij} - v_i|}$ $(j = 1, \ldots 4)$ are unit edge vectors emitting from the vertex v_i. Norms $|v_{ij} - v_i|$ and $|e_{i1} - e_{i3}|$, $|e_{i2} - e_{i4}|$ can be computed in each iteration. Then the angle energy term is:

$$E_{\text{angle}} = \sum_{i=1}^{|V|} \left(\frac{e_{i1} - e_{i3}}{|e_{i1} - e_{i3}|} \cdot \frac{e_{i2} - e_{i4}}{|e_{i2} - e_{i4}|} - \cos\theta_0 \right)^2 + \sum_{i=1}^{|V|} \sum_{j=1}^{4} \left(e_{ij} - \frac{v_{ij} - v_i}{|v_{ij} - v_i|} \right)^2 \tag{3}$$

Bottom curve energy. The bottom curve is planar and geodesic. The curve vertices lie on the XY-plane.

$$\sum_{b \in \text{bottom\_polyline}} (v_b \cdot [0, 0, 1])^2 = 0$$

We apply the geodesic energy Eq. (2) to any three consecutive vertices v_{bl}, v_b, v_{br} of the bottom curve. However, since the valence of the boundary vertices is 3, the vertex normal n_b is not as clearly defined as any regular vertex stars in Eq. (1). We thus extend the bottom curve with additional rows of vertices so that the original boundary vertices are interior (Fig. 5c, red curve), and the planar vertex stars, vertex normal Eq. (2), and geodesic curves are well defined:

$$\sum_{b \in \text{bottom\_polyline}} (n_b \cdot [(v_{bl} - v_b) \times (v_{br} - v_b)])^2 = 0$$

After suitable convergence is achieved, these artificial rows of vertices can be removed, and the geodesic property of the assigned bottom boundary curve is preserved. This bottom curve energy term is combined as

$$E_{\text{bottom}} = \sum_{b \in \text{bottom\_polyline}} \left((v_b \cdot [0, 0, 1])^2 + (n_b \cdot [(v_{bl} - v_b) \times (v_{br} - v_b)])^2 \right) \quad (4)$$

Symmetry energy. The left and right areas of the AAG-web are symmetric with respect to the central *YZ*-plane, so the left vertices v_{left} and right vertices v_{right} form the energy term

$$E_{\text{sym}} = \sum \left((v_{\text{left}} - v_{\text{right}})^2 \times [1, 0, 0] \right)^2 \quad (5)$$

Fairness energy. A regularizer for any three consecutive vertices of a polyline allows for obtaining smoother polylines. It works as a weighted fairness term

$$E_{\text{fair}} = \sum_{i \in \text{poly}} (2v_i - v_{il} - v_{ir})^2 \quad (6)$$

Target function. The objective function for our AAG-web is a combination of (1)-(6) as

$$E = E_{\text{Anet}} + E_{\text{geo}} + E_{\text{angle}} + 10 \cdot E_{\text{bottom}} + E_{\text{sym}} + \omega E_{\text{fair}} \quad (7)$$

where $\omega (< 1)$ is a smaller weight enabled during the optimization and disabled in the final optimization steps to ensure convergence. To make sure the property of the bottom curve is highly satisfied, we choose a high weight (i. e. 10) for this term. We use the guided projection method (Tang et al. 2014), which is a Gauss-Newton method, to get the solver of Eq. (7). The algorithm is implemented in Python and tested on an Intel Xeon E5-2687W 3.0 GHz processor.

The densely optimized AAG-web (Fig. 6a) is converted into NURBS geometry through interpolation. Alternating curves of A and G are selected (b) to generate a tri-hex kagome pattern, which reduces density while improving constructive and load-bearing qualities (see Sec. 3.1 and 3.2). The grid is then cropped along geodesic boundaries (to simplify fabrication), which align with the grid on the bottom and sides but follow a misaligned geodesic path along the ridge, to closely offset to the symmetry plane. This NURBS geometry model is used to set up a parametric model (c) in Rhinoceros 3D – Grasshopper, and develop construction strategies, offsets, thicknesses, details, and materiality to a high level. The final design of the Asymptotic Geodesic Hybrid Timber Gridshell is based on three symmetric AAG webs that form a negatively curved vault.

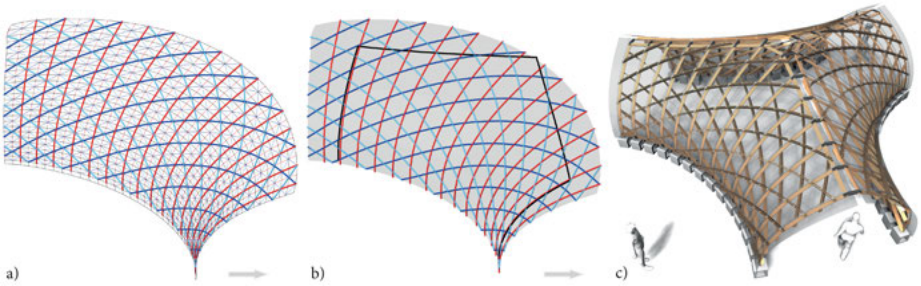

Fig. 6: The optimized mesh (a) is converted into a NURBS surface and curves through interpolation (b). Specific asymptotic and geodesic curves are selected to generate a tri-hex pattern. The curves and surface are cropped and processed, to create a detailed architectural model (c).

3 Construction Development

Finger jointed ash lamellas were chosen as the building material due to their outperforming properties of strength and elasticity (Kovryga et al. 2020). To avoid any waste of resources, the thinnest cross-sections supplied by the sawmill of 25 × 100 mm were purchased and simply split to create 2 × 12 × 100 mm planks. The choice of material and cross-section became a decisive driver for the design geometry, as it naturally limits the minimum radii for bending ($r_{\min} = 1.7$ m) and maximum twist ($\beta_{\max} = 60°/\text{m}$).

3.1 Timber Network and Joints

We create a tri-hex web in which geodesic planks connect to the midpoints of each asymptotic beam (Fig. 7i, 8d). This has three decisive advantages for construction and load-bearing behavior: 1) The geodesic planks can be assembled independently, either in the flat or curved stage of the erection process. They are connected simply with a steel screw to the coupling blocks of asymptotic beams. 2) The geodesic planks are used as locking mechanism of the kinetic erection process. During erection, the geodesic planks slide between the asymptotic layers and allow for a change in geometry. Once the final design shape is reached, the geodesics are fixed and brace the structure. 3) The geodesic planks are interwoven between top and bottom asymptotic beams at mid-points, and thus half the buckling length of both the asymptotic beams, as well as the geodesic planks themselves.

The timber is cut to length and drilled with minimal holes to allow reuse. This low-tech fabrication is achieved by assembling the three families of planks in three separate layers, with asymptotic beams on top and bottom and geodesic planks in between. Each asymptotic beam is constructed from two planks, which are individually bent and coupled with 24 mm blocks. These *coupled asymptotic beams* have three advantages:

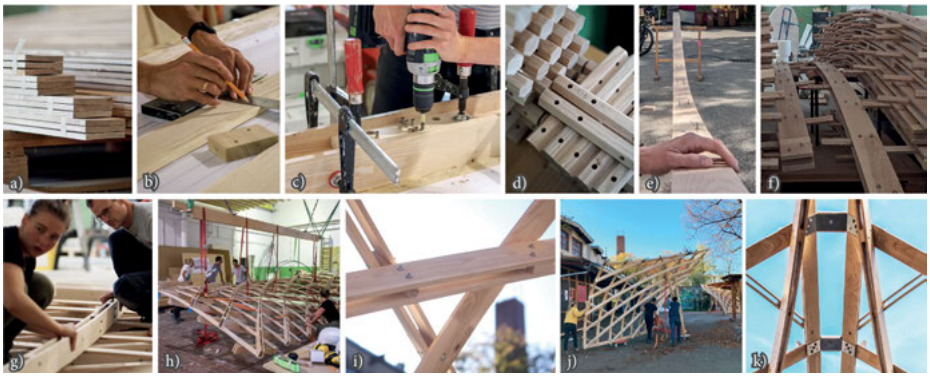

Fig. 7: Top Row: Prefabrication. 12 × 100 mm planks (a) are marked (b), drilled (c), and coupled with 24 mm studs (d) into pre-bent (e) beams (f). This process embeds the geodesic curvature. Bottom Row: Assembly and Erection. The asymptotic beams and geodesic planks are interlaced into flat segments (g), and deformed into the doubly curved shape (h). The combination of asymptotic and geodesic planks (i) creates a stiff shell, that is transported (j) and assembled (k) on site.

1) The two sibling planks are pre-drilled individually, incorporating slight differences in the node-to-node distance. This allows us to embed the geodesic curvature during prefabrication (Fig. 7f). 2) The planks can be deformed individually but, after they are coupled, act as one strong beam with high lateral bending stiffness. 3) The parallel layout of planks at 24 mm distance allows a centric connection of top and bottom asymptotic beam using 22 cm long (24 × 24 mm) hexagonal studs (Fig. 7d).

3.2 Prefabrication and Assembly

The prefabrication is simple (Fig. 7). The ash planks (a) are first marked by hand (b) and cut to the right length. Groups of three identical planks (for three shells) are then aligned and tightly clamped (to overcome individual warping due to humidity and drying of the material) and pre-drilled using templates (c). The asymptotic beams are assembled each from two individual planks with 24 mm studs (d) in between. The planks are laid across two stands so that they naturally bend and sag into a curved shape, until the pre-drilled holes align. The two planks are then coupled at each stud with two steel bolts (e). With this method, 66 pre-curved asymptotic beams were prefabricated and stored to wait for further processing (f).

As a next step, the asymptotic beams and geodesic planks are *assembled* flat on the ground (g) into the three-layered tri-hex web. The top and bottom asymptotic beams are connected loosely (to still allow some rotation) through the long studs, while the geodesics are simply slid in between (without connections). The flat segment is then hoisted up (h) and elastically deformed into the design shape (i). During this process, the geodesic planks shift through the grid, the asymptotic beams are twisted, and the

Fig. 8: Completed timber gridshell. Top Row: a) Precast concrete blocks with steel supports. b,c) Birds-eye view of the timber gridshell without cover. d) Inside the Timber Vault. Bottom Row: Polycarbonate panels are tailored with concave edge (e), and installed using aluminum mullions along the geodesic directions (f), to create a smooth, transparent skin (g).

AA-joints slightly rotate into the final 60° angle. The final geometry is fixed by adding geodesic planks at upper and lower boundaries and fixing all bolts for asymptotic and geodesic planks. These stiff shell elements are transported to the building site (j) and combined along the roof ridge with steel blades (k). The timber gridshell (Fig. 8) is supported by 42 precast concrete blocks (14 for each shell) to resist wind suction and horizontal thrust. The shell elements are fixed with vertical steel bolts (a) that allow individual height adjustment to overcome construction tolerances. A *curved transparent cover* was installed (Fig. 8 e-f) to protect the wood from weathering and create a sheltered space. 13 strips of 10 mm thick polycarbonate multi-skin sheet are clamped and bent along the geodesic directions to form a semi-discrete skin. Each panel is tailored with a long concave edge (e) to accommodate the negative curvature. The AAG Timber Vault is the first architectural application that combines asymptotic and geodesic planks in a triangulated web. The structure consists of three shells covering an area of 60 m^2. Each shell weighs approx. 300 kg for timber, 30 kg for steel screws and plates, and 40 kg for façade panels and aluminum profiles. This equates to a total of 1100 kg for 100 m^2 roof area (approx. 11 kg/m^2).

4 Structural Performance

The design of the Timber Vault was driven by structural criteria. To activate a shell behavior, the grid was designed with a vaulted shape, linear supports, and was adjusted to its highest possible double curvature without exceeding the minimal bending radii

of lamellas. The tri-hex grid with constant node angles ensures a homogenous edge length and additional bracing effect to increase the overall stiffness.

4.1 Structural Analysis

During the planning process, multiple load combinations were considered in detail, combining self-weight, snow load (full-span/half-span), wind load from three directions, as well as the residual stresses caused by the elastic deformation process during assembly (see Sec. 3.2). In this paper, we can only shortly highlight the full-span load and physical test results. For this article, the structural performance of the timber gridshell was evaluated using the Finite Element (FE) software Karamba 3D (Preisinger 2013), using a linear solver to simulate the structural behavior. All members are modelled using 2-node beam elements with 6 DOFs at each node. The connections are assumed to be all rigid, except for the geodesic connection, which allows rotation around local z. An elastic material model is used for the ash timber with Young's modulus of 14000 N/mm^2 and bending strength of 50 N/mm^2, obtained from the literature (DIN EN 338 2016) and confirmed by preliminary material testing. The boundary is fixed in three directions as hinge supports at every end of the geodesic lamellas.

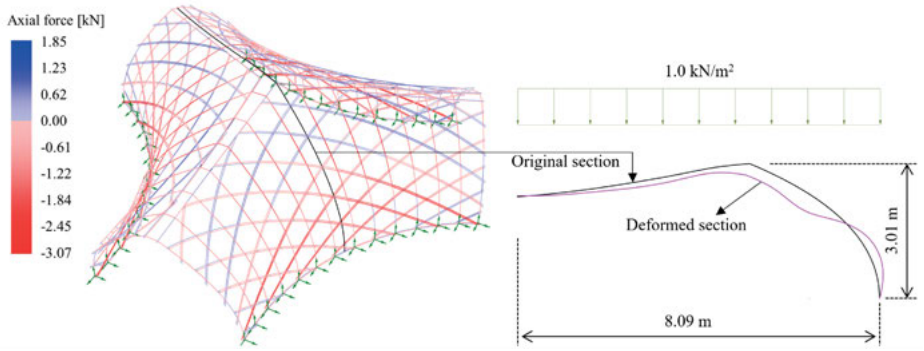

Fig. 9: Axial force (left) and section deformation mode (right) of the asymptotic-geodesic timber vault under self-weight and a full-span homogenous load of 1.0 kN/m^2; deformation is scaled by 80.

Full-span distributed load. To visualize the overall load-bearing behavior, we simulate the gridshell under its self-weight (without residual stress) and a full span homogenous load of 1.0 kN/m^2 on the horizontal projection plane. The external surface load is discretized and applied to the joints of the structure. The structural behavior (Fig. 9) can be described as an "inverted dome". The shell's top part deforms inwards. Due to the negative curvature, this deflection stretches the upper members in the horizontal direction and generates tension forces in the asymptotic beams. On the contrary, the

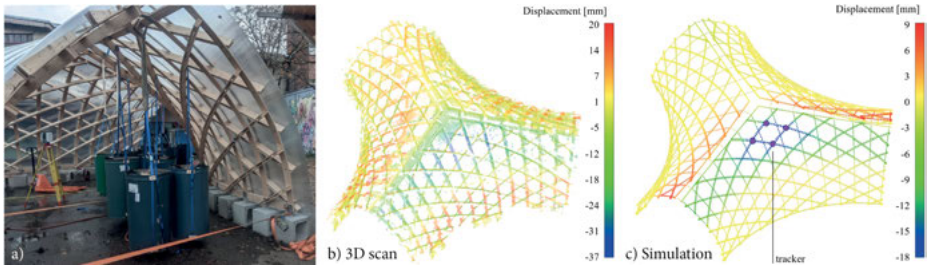

Fig. 10: Structural test under an asymmetric load of 26 kN. a) 13 barrels were filled with up to 200 l of water. b) The scanned point cloud illustrates the vertical deflections, which were compared with the simulation result (c).

shell's lower part deforms outwards, shortening the asymptotic lamellas and leading to compression. The compression in the geodesic planks decreases in the lower part, as they resist the scissor-distortion of the asymptotic grid. This arrangement allows the structure to transfer loads in a membrane-like force within the shell. The upright asymptotic planks provide out-of-plane stiffness, while the flat geodesic planks provide in-plane stiffness and reduce the buckling length.

4.2 Load Tests

To assess the loading capacity of the built structure, we conducted several physical loading tests on the constructed prototype, including one-point loading, local region loading, and one-shell asymmetric loading. The one-shell asymmetric loading is shown in Fig. 10. To avoid the supports sliding on the ground, we used six belts as horizontal ties between opposite supports. Gradually, 13 barrels were each filled with 200 liters of water, reaching a total of 26 kN vertical load distributed on 13 loading points (Fig. 10a). During this test, no failure, cracking or sudden movement of the structure was recorded. The structure was scanned using both a point cloud (Fig. 10b) and individual trackers. The deformation modes from the load test are well compatible with the results of the FE simulation. The average vertical deflection of four joints (marked with purple in Fig. 10c) is measured as 16 mm in the FE simulation and 31 mm in the scanning. Three factors may account for the magnitude difference. First, the material properties used in the FE simulation are only an estimation of the material properties of the real structure (Sec. 4.1). Second, unlike the FE simulation, the supports were not fully fixed in the load testing (as the horizontal belts were able to stretch). Third, the joints in the real structure are not completely rigid due to construction tolerance.

5 Conclusion

In this paper, we implemented the design and construction of triangulated doubly curved AAG gridshells from standardized planks of timber, with the goal to enable a circular use of building material. To enable an efficient computational workflow, we first designed negatively curved rotational surfaces to then initialize the discrete optimization of specific constraints that would simplify fabrication and improve structural performance. The dependency between geometric parameters and material properties played a decisive role in the design process, which is seeking a beneficial shape for structure and supports, a balance of curvature and elasticity, a clean arrangement of the 3-web to accommodate façade and boundaries, and well-resolved layering and detailing of planks. This iterative process yielded a triple symmetric negatively curved AAG-Vault with constant 60° nodes. The use of repetitive joints was significant to streamline fabrication and create a homogenous network with structural and aesthetic qualities. The construction process takes advantage of the global kinetic behavior of asymptotic grids, and thus poses challenges due to the residual stress, which limits the plank thickness, causes relaxation and creep, and affects the building accuracy. Physical tests and structural simulation were compared via 3D scan, to validate the load-bearing efficiency of this system. The accuracy of results, however, is dependent on the precise knowledge of specific material properties, as well as the stiffness of supports and joints. An official proof of structural stability for this structure has been completed following Euro-Code 5. The system will further be developed with industrial partners (Holzbau Amann and Erhard Brandl) to create economic and ecological prefabricated shells for modular timber construction. The research will address questions of relaxation and accuracy, supports and assembly on site, as well as climatic behavior and maintenance with changing humidity. An in-depth publication on structural behavior and applicability to larger spans is in progress. Finally, we plan to disassemble the gridshell after 2 years, survey the quality and creep of planks, and evaluate their reuse in a new construction cycle.

Acknowledgements

The research has been supported by the University Grants Committee (UGC) of Hong Kong, Early Career Scheme (RGC Ref No. 27604721), the Special Projects Fund, HKU DoA, the Professorship of Structural Design, TUM, as well as our industry partners Holzbau Amann and Metallbau Erhard Brandl. We thank the students of the course Structural Research at TUM and colleagues at TUM, and HKU for their joint effort in modelling, prefabricating and erecting the Timber prototype. We acknowledge Kayser+Böttges / Barthel+Maus, BIGA, Máté Péntek and Jörg Rehm for their consultations in structure, timber, wind and fire safety.

References

DIN EN 338 (2016). DIN EN 338: Bauholz für tragende Zwecke – Festigkeitsklassen. Berlin.

Finsterwalder, S. (1897). Mechanische Beziehungen bei der Flächen-Deformation. In *Jahresbericht der Deutschen Mathematiker-Vereinigung,* vol. 6., 43–90.

Haskell, C., Montagne, N., Douthe, C., Baverel, O., Fivet, C. (2021). Generation of elastic geodesic gridshells with anisotropic cross sections. *Int. J. Space Struct.* 36(4), 294–306.

Jiang, C., Wang, C., Schling, E., Pottmann, H. (2020). Computational design and optimization of quad meshes based on diagonal meshes. In *Advances in Architectural Geometry 2020.*

Kovryga, A., Stapel, P., van de Kuilen, J. W. G. (2020). Mechanical properties and their interrelationships for medium-density European hardwoods, focusing on ash and beech. *Wood Material Science & Engineering* 15(5), 289–302.

Natterer, J., Burger, N., Müller, A. (2000). Holzrippendächer in Brettstapelbauweise – Raumerlebnis durch filigrane Tragwerke. *Bautechnik* 77(11), 783–92.

Pottmann, H., Asperl, A., Hofer, M., Kilian, A. (2007). *Architectural geometry.* Bentley Institute Press.

Pottmann, H., Huang, Q., Deng, B., Schiftner, A., Kilian, M., Guibas, L., Wallner, J. (2010). Geodesic Patterns. *ACM Trans. Graphics* 29 (4).

Preisinger, C. (2013). Linking Structure and Parametric Geometry. *Archit. Design* 83(2), 110–13.

Sauer, R. (1937). *Projektive Liniengeometrie.* Walter de Gruyter&Co.

Sauer, R. (1970). *Differenzengeometrie.* Berlin, Heidelberg: Springer Berlin Heidelberg.

Schikore, J. (2023). Compliant Grids. Theory, Design and Realization. Doctoral Dissertation (to be published). Technical University of Munich, Munich. Chair of Structural Design.

Schikore, J., Schling, E., Oberbichler, T., Bauer, A. M. (2020). Kinetics and Design of Semi-Compliant Grid Mechanisms. In *Advances in Architectural Geometry 2020,* 108–29.

Schling, E. (2018). Repetitive Structures. Design and Construction of Curved Support Structures with Repetitive Parameters. Dissertation. Technical University of Munich, Chair of Structural Design. DOI: 10.14459/2018md1449869

Schling, E., Kilian, M., Wang, H., Schikore, J., Pottmann, H. (2018). Design and Construction of Curved Support Structures with Repetitive Parameters. In *Advances in Architectural Geometry 2018,* 140–65.

Schling, E. and Z. Wan. (2022). A geometry-based design approach and structural behaviour for an asymptotic curtain wall system. *J. Build. Eng.* 52, 104432. DOI: 10.1016/j.jobe.2022.104432

Schling, E., Wang, H., Hoyer, S., Pottmann, H. (2022). Designing asymptotic geodesic hybrid gridshells. *Computer-Aided Design* 152 (0010-4485), p. 103378. DOI: 10.1016/j.cad.2022.103378

Soriano, E. (2017). Low-Tech Geodesic Gridshell: Almond Pavilion. *Archi DOCT* 4(2), 29–40.

Tang, C., Kilian, M., Bo, P., Wallner, J., Pottmann, H. (2016). Analysis and design of curved support structures. In *Advances in Architectural Geometry 2016,* 8–23.

Tang, C., Sun, X., Gomes, A., Wallner, J., Pottmann, H. (2014). Form-finding with polyhedral meshes made simple. *ACM Trans. Graph.* 33(4), 1–9.

Wan, Z., Schling, E. (2022). Structural principles of an asymptotic lamella curtain wall. *Thin-Walled Structures* 180, p. 109772. DOI: 10.1016/j.tws.2022.109772

Wang, Hui and H. Pottmann. (2022). Characteristic parameterizations of surfaces with a constant ratio of principal curvatures. *Computer Aided Geometric Design* 93, p. 102074.

Weinand, Y. and C. Pirazzi. (2006). Geodesic Lines on Free-Form Surfaces. Optimized Grids for Timber Rib Shells. With assistance of IBOIS. In *World Conference in Timber Engineering WCTE.*

Wunderlich, W. (1951). Zur Differenzengeometrie der Flächen konstanter negativer Krümmung. In *Österreich. Akad. Wiss. Math.-Nat. Abt. IIa* 160, 39–77.